Compression as a path to simplification: Models of collective neural activity

Luisa Ramirez[1,2] and William Bialek[2,3]
[1] *Departamento de Física, Universidade Federal de Minas Gerais, CEP 31270–901 Belo Horizonte, Minas Gerais, Brasil*
[2] *Joseph Henry Laboratories of Physics, and Lewis–Sigler Institute for Integrative Genomics, Princeton University, Princeton, NJ 08544*
[3] *Initiative for the Theoretical Sciences, The Graduate Center, City University of New York, 365 Fifth Ave., New York, NY 10016*
(Dated: December 30, 2021)

Patterns of activity in networks of neurons are a prototypical complex system. Here we analyze data on the retina to show that information shared between a single neuron and the rest of the network is compressible, through a combination of the information bottleneck and an iteration scheme inspired by the renormalization group. The result is that the number of parameters needed to describe the distribution of joint activity scales with the square of the number of neurons, even though the interactions are not well approximated as pairwise. Our results also show that the shared information is essentially equal to the information that individual neurons carry about natural visual inputs, which has implications for the structure of the neural code.

arXiv:2112.14334v1 [q-bio.NC] 28 Dec 2021

The last decade has seen enormous growth in our ability to monitor, simultaneously, the functional activity of many degrees of freedom in living systems. Examples range from the expression levels of many genes in a single cell [1–4] to the electrical activity of many neurons in the brain [5–10] and the movements of all the individual organisms in a flock or swarm [11]. In order to understand these experiments we need a theoretical framework that tames the combinatorial explosion of potential complexity. In physics we are accustomed to using very simple models to describe systems with many degrees of freedom, but it is not clear why or how this success can be transferred to the more complex biological context.

We can identify several different reactions to the increased dimensionality of the available experimental data. One view, inspired by the success of modern AI, embraces complex models such as deep neural networks, emphasizing that successful predictions are possible even when the number of parameters in our models far exceeds the number of data points [12]. The opposite view is that high dimensional data may lie on lower dimensional manifolds, so that the search for these manifolds becomes the central problem of data analysis [13, 14]. An intermediate approach focuses on the fact that complex models often have a characteristic geometry in parameter space, where some combinations of parameters are essential for successful prediction and others are not [15, 16]. Other approaches are more explicitly connected to ideas from statistical physics, including the construction of maximum entropy models that are consistent with low–order correlations [17–23] and the search for scaling behaviors that might point toward models described by a fixed point of the renormalization group [24–26]. Here we explore a new approach to simplification, the compressibility of interactions [27], and apply this idea to the electrical activity of neurons in large networks.

In each small window of time we define a binary or Ising variable σ_i that marks whether neuron i is active ($\sigma_i = +1$) or silent ($\sigma_i = 0$). Although there are many formulations, we pose the problem of understanding as building a model for the joint probability distribution of all these variables, $P(\{\sigma_i\})$. To focus on the interactions, we consider the distribution for the state of one variable σ_0 given the state of the rest of the network, $P(\sigma_0|\{\sigma_j\})$. If we can understand this distribution for each possible choice of σ_0, we will have understood the whole network.

If there are K neurons in the set $\{\sigma_j\}$, then in principle we need 2^K different values of the "effective field"

$$h_{\rm eff}\left(\{\sigma_j\}\right) = \ln\left[\frac{P\left(\sigma_0 = 1|\{\sigma_j\}\right)}{P\left(\sigma_0 = 0|\{\sigma_j\}\right)}\right]. \tag{1}$$

A conventional simplification is to expand $h_{\rm eff}$ in a series,

$$h_{\rm eff}\left(\{\sigma_j\}\right) = h_0 + \sum_j J^{(2)}_{0j}\sigma_j + \frac{1}{2}\sum_{j,k} J^{(3)}_{0jk}\sigma_j\sigma_k + \cdots . \tag{2}$$

Stopping with the second term corresponds to allowing only pairwise interactions in the effective Hamiltonian $H = -\ln P$, and gives a description of $P(\sigma_0|\{\sigma_j\})$ with $K+1$ rather than 2^K parameters.

Compressibility of interactions means that we do not need to keep every detail of the network state $\{\sigma_j\}$ in order to make reliable predictions of the effective field. Concretely, this means compressing $\{\sigma_j\} \to \tilde{\sigma}$, where $\tilde{\sigma}$ takes on M states, with $M \ll 2^K$. To measure the quality of the compression we ask how much of the mutual information is captured, and optimize, so that we are solving the problem

$$\max_{\{\sigma_j\}\to\tilde{\sigma}} I\left(\sigma_0;\tilde{\sigma}\right). \tag{3}$$

This maximum depends on the number of states in $\tilde{\sigma}$, $I_{\rm max}(M)$, and can be compared with the full mutual information $I(\sigma_0;\{\sigma_j\})$. If we can achieve $FI =$

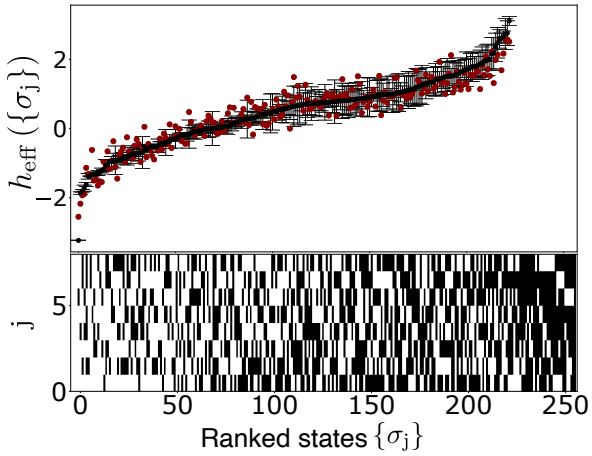

FIG. 1: The effective field $h_{\rm eff}(\{\sigma_j\})$ as a function of the states $\{\sigma_j\}$, in rank order. Mean, with error bars estimated from the standard deviation across random halves of data (black), and best least squares fit to Eq (2) truncated at third order (red). Ranked states are represented in the figure below the trace, with black indicating that a neuron is "on," $\sigma_j = 1$. States at far right are not observed in data.

$I_{\rm max}(M)/I(\sigma_0;\{\sigma_j\}) \approx 1$ for small M even at large K, then we have tamed the combinatorial explosion.

To solve the optimization problem in Eq (3), we start with some random assignment $\{\sigma_j\} \to \tilde{\sigma}$ and compute

$$P(\sigma_0;\tilde{\sigma}) = \sum_{\{\sigma_j\}\in\tilde{\sigma}} P(\sigma_0|\{\sigma_j\})\,P(\{\sigma_j\}), \quad (4)$$

$$P(\tilde{\sigma}) = \sum_{\{\sigma_j\}\in\tilde{\sigma}} P(\{\sigma_j\}), \quad (5)$$

and $P(\sigma_0|\tilde{\sigma}) = P(\sigma_0;\tilde{\sigma})/P(\tilde{\sigma})$ as usual. Then for each particular state we can compute the Kullback–Leibler divergence

$$D_{KL}(\{\sigma_j\};\tilde{\sigma}) = \sum_{\sigma_0} P(\sigma_0|\{\sigma_j\}) \ln\left[\frac{P(\sigma_0|\{\sigma_j\})}{P(\sigma_0|\tilde{\sigma})}\right], \quad (6)$$

and reassign

$$\{\sigma_j\} \to \arg\min_{\tilde{\sigma}} D_{KL}(\{\sigma_j\};\tilde{\sigma}). \quad (7)$$

Iterating, we arrive at a mapping $\{\sigma_j\} \to \tilde{\sigma}$ that maximizes $I(\sigma_0;\tilde{\sigma})$. This is the zero temperature or hard clustering limit of the information bottleneck [28].

To see how this works in practice, we look at experiments on the response of $N = 160$ retinal ganglion cells to naturalistic movies [21]. In these data, $\sigma_i = 1(0)$ corresponds to the presence (absence) of an action potential from neuron i in a window of duration $\Delta\tau = 20$ ms. We choose one neuron in the population as σ_0, and then order the remaining neurons by their mutual information $I(\sigma_0;\sigma_i)$. In order to be sure that we can calibrate the fraction of information that we capture, we focus on smaller groups of K neurons. Choosing K involves a trade–off between statistical reliability and compression significance: at larger K it is more significant to find a successful compression, but it is more difficult to make reliable statistical inferences. As we will see, $K = 8$ provides an effective compromise.

Consider the $K = 8$ neurons that share the most information with some particular σ_0. Figure 1 shows the effective field $h_{\rm eff}$ as function of the state $S_1 = \{\sigma_j\}$ for this example. We note that 218 of the 256 possible states are visible in the data. If we try to describe these data through Eq (2), then even including terms up to $J^{(3)}$ leaves considerable scatter.

To compare the performance of compression methods with the performance of series expansions, we recall that a model for the probability distribution P provides an encoding of the data, with code words of length $\ell = -\log_2 P$ bits [29]; the shortest mean code length $L_{\rm min}$ is the entropy of the true distribution, and approximate models give longer codes. In this case we are building a code for the binary variable σ_0 conditional on the state of the other K neurons. If we have an approximate model for $h_{\rm eff}(\{\sigma_j\}) \approx \hat{h}_{\rm eff}(\{\sigma_j\})$, the mean code length

$$L_{\rm approx} = -\frac{1}{\ln 2}\langle\sigma_0\hat{h}_{\rm eff}(\{\sigma_j\})\rangle + \left\langle \log_2\left[1+e^{\hat{h}_{\rm eff}(\{\sigma_j\})}\right]\right\rangle, \quad (8)$$

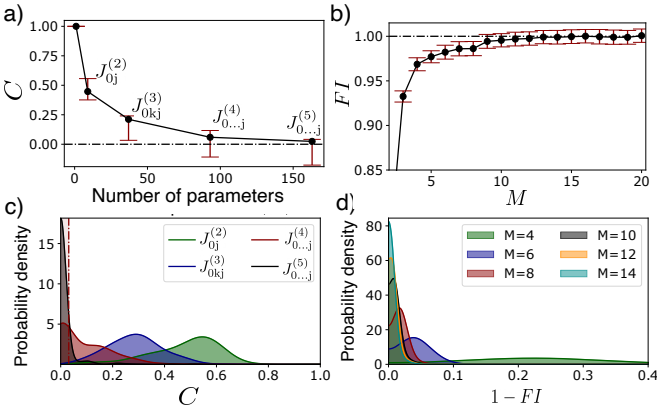

FIG. 2: Series expansions vs compression. (a) Coding cost [Eq (9)] as a function of the number of parameters for the series expansion in Eq 2. Black points from analysis with all data, error bars are standard deviation across random choices of learning from 60% of the data and testing on the remaining 40%. (b) Fraction of mutual information captured as a function of the number of states M in the compressed representation $\tilde{\sigma}_i$. Error bars from analyses of random subsets of the data. (c) Coding cost probability density over all possible choices of σ_0. Each curve correspond to a different order truncation, $J^{(i)}_{0j}$, of the series expansion [Eq.2]. (d) Probability density of the fractional information over all possible choices of σ_0. Each curve correspond to a different value of M. We used a weighted-KDE method for the inference of the probability densities, considering the measured error bars of each choice of σ_0.

where $\langle \cdots \rangle$ is an average over the observed states of the system. The most naive approximation ignores interactions, assigning the same effective field to all states, and this "independent" code has length $L_{\rm ind}$. A natural measure of coding cost is then

$$C = (L_{\rm approx} - L_{\rm min})/(L_{\rm ind} - L_{\rm min}), \tag{9}$$

which ranges between zero and one. For the case where we do a proper compression $\{\sigma_j\} \to \tilde{\sigma}$, then $C = 1 - FI$, where FI is the fraction of the mutual information that we capture (see above), but the coding cost is defined more generally, e.g. in the truncated series expansions of Eq (2). In Figures 2a and b we compare the optimal compressions with the series expansion, and find that compression into $M \sim 10$ states performs as well as including 163 parameters to describe 5th order interactions.

To check that these results do not depend on our choice of the central neuron σ_0, in Figs 2c and d we show the distribution of coding cost and fractional information across these choices. We see in Fig 2c that even getting within ten percent of the optimum across the majority of neurons requires extending the series expansion to fifth order. In contrast, Fig 2d shows that by compressing into $11 - 15$ states we achieve a code that captures all but a few percent of the available mutual information, for all neurons in the population. To summarize, in this network we can describe the influence of $K = 8$ neurons on one neuron using just $M = 11 - 15$ parameters, but this most efficient description does not correspond to a simple choice of pairwise or other low order interactions.

Estimates of mutual information come with errors, and so statements about the number of states needed to capture a given fraction of the information also have uncertainty. For each choice of σ_0 and $\{\sigma_j\}$ out of the network, estimates of FI are accompanied by an error $\Delta_{FI}(\sigma_0, \{\sigma_j\})$, and as a global measure Δ_{FI} we take the median of these errors. If we choose a fixed number of states M for the compression, then across all choices of σ_0 and $\{\sigma_j\}$ we will find a fraction D_{FI} for which the estimate of FI is larger than $1 - \Delta_{FI}$, i.e. the information captured is within errors of the information available.

We can do this analysis not just for interactions between a single cell σ_0 and its K most informative partners, $S_1 = \{\sigma_1, \ldots, \sigma_8\}$, but also for interactions with successively less informative groups $S_l = \{\sigma_{k(l-1)+1}, \ldots, \sigma_{k(l-1)+k}\}$, and the results are the same. Figure 3a (blue) shows the fraction of cells and groups for which which we can capture the available information within errors with M states, and this fraction is computed across the first eight groups of eight neurons each, for all $N = 160$ choices of σ_0. Note that with $l = 8$ we are covering $0.4N$ of the cells in the entire population, and that $I(\sigma_0; S_l)$ is within error bars of zero for $l > 8$. We conclude that in 90% of all the relevant groups we achieve essentially perfect compression with $M^* \sim 11$ states.

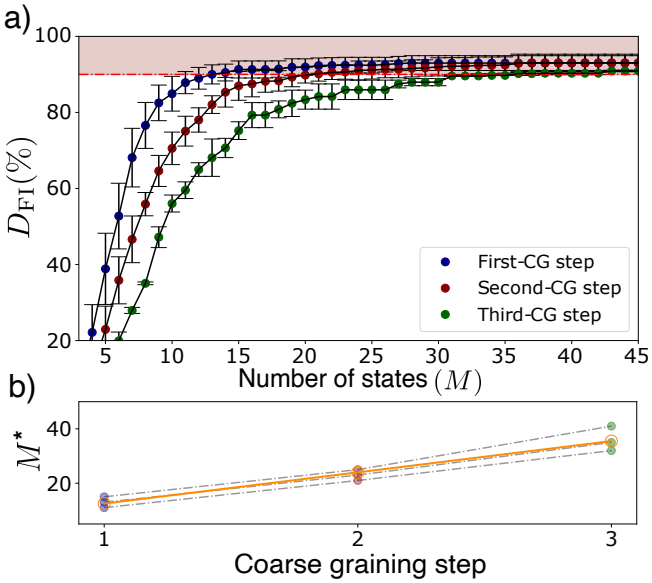

FIG. 3: (a) Fraction of cells σ_0 and groups $\{\sigma_j\}$ such that compression into M states captures the available mutual information, within error bars. Successive coarse graining steps as described in the text. We define M^* as the minimum number of states needed to achieve complete compression in 90% of the cases. b) Minimum number of states M^* as a function of the coarse graining step. Dashed curves (grey) correspond to different compression iterations, which vary because of noise in our estimates, together with linear fit (orange).

The compression $\{\sigma_j\} \to \tilde{\sigma}$ is reminiscent of the block spin construction in the renormalization group (RG) [30, 31]. We recall that block spins are coarse–grained variables that replace groups of spins. In the present context, it is important to remember that coarse–graining can be thought of as data compression, and vice versa. By analogy with the RG, then, we would like to do iterative compression.

Concretely, we are focused on a variable σ_0 and have ordered the remaining variables σ_j by their mutual information with σ_0. Our first coarse graining step has been to take these variables in groups of $K = 8$, and compress according to the solution of the optimization problem in Eq (3), which gives us

$$\begin{aligned} \{\sigma_1, \sigma_2, \cdots, \sigma_8\} &\to \tilde{\sigma}_1^{(1)} \\ \{\sigma_9, \sigma_{10}, \cdots, \sigma_{16}\} &\to \tilde{\sigma}_2^{(1)} \\ &\cdots \ , \end{aligned} \tag{10}$$

where each of the variables $\tilde{\sigma}_n^{(1)}$ has M states. To iterate, we take pairs of these variables and compress again, e.g.

$$\left(\tilde{\sigma}_1^{(1)}, \tilde{\sigma}_2^{(1)}\right) \to \tilde{\sigma}_1^{(2)}, \tag{11}$$

where again the mapping is chosen to maximize the mutual information $I(\sigma_0; \tilde{\sigma}_1^{(2)})$. We can keep iterating,

$$\left(\tilde{\sigma}_1^{(2)}, \tilde{\sigma}_2^{(2)}\right) \to \tilde{\sigma}_1^{(3)}, \tag{12}$$

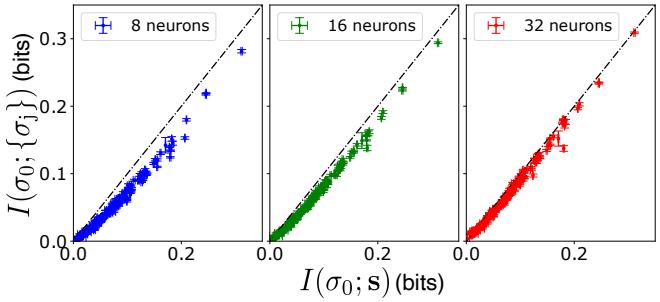

FIG. 4: Information shared with the network vs information about the stimulus. Plot corresponds to the first (blue, 8 neurons), second (green, 16 neurons) and third (red, 32 neurons) coarse graining steps. Estimates and errors as in Ref [32].

always with the same principle of choosing the compression that maximizes the mutual information with σ_0.

It is not surprising that successive stages of compression or coarse graining require more states to capture all the available mutual information, as shown in Fig 3a. What is surprising is that the minimal number of states M^* seems to grow linearly rather than exponentially as we proceed through multiple stages, as seen in Fig 3b. After three stages, we are describing the interactions of σ_0 with 32 other cells using only $M_3^* = 32$ states. The linear growth of M^* with the number of neurons is explicit evidence that we have tamed the combinatorial explosion, combining the compressibility of interactions with an RG–inspired iteration scheme.

The scaling of M^* is what we might expect in a model with pairwise interactions, or if single neurons coupled only to the total activity of other neurons, but neither of these simplifications is correct. Rather than digging into the details of the compressed states, which will be different for every group of cells, we can ask about the amount of information that we identify as shared between single neurons and their most informative partners, $I(\sigma_0;\tilde{\sigma})$. Since the neurons we are analyzing are the output neurons of the retina, a natural comparison is between this information and the information that individual neurons carry about the visual stimulus, $I(\sigma_0;\mathbf{s})$. The experiments in Ref [21] include repeated presentations of the same movie, so we can estimate $I(\sigma_0;\mathbf{s})$ directly without any assumptions about which features of the visual stimulus are being encoded, following [32].

Figure 4 shows that as we consider larger groups of neurons, the information that single neurons share with the network, $I(\sigma_0;\tilde{\sigma})$, approaches the information that these neurons carry about the visual stimulus, $I(\sigma_0;\mathbf{s})$, reaching equality within (small) error bars. This has a surprising consequence for our understanding of neural coding. The K neurons that go into defining $\tilde{\sigma}$ carry some information about the visual stimulus, $I(\{\sigma_j\};\mathbf{s})$, and adding the extra neuron σ_0 provides additional information

$$\Delta I(\sigma_0;\mathbf{s}) = I(\{\sigma_j\},\sigma_0;\mathbf{s}) - I(\{\sigma_j\};\mathbf{s}). \quad (13)$$

Following Ref [33] we have

$$\Delta I(\sigma_0;\mathbf{s}) = I(\sigma_0;\mathbf{s}) + I(\sigma_0;\{\sigma_j\}|\mathbf{s}) - I(\sigma_0;\{\sigma_j\}), \quad (14)$$

where $I(\sigma_0;\{\sigma_j\}|\mathbf{s})$ is the (average) mutual information between σ_0 and the network given that visual stimulus is known. The fact that we achieve lossless compression means we can replace $I(\sigma_0;\{\sigma_j\})$ by $I(\sigma_0;\tilde{\sigma})$, and Fig 4 tells us that $I(\sigma_0;\tilde{\sigma}) = I(\sigma_0;\mathbf{s})$, so that

$$\Delta I(\sigma_0;\mathbf{s}) = I(\sigma_0;\{\sigma_j\}|\mathbf{s}). \quad (15)$$

If neurons respond independently to the visual inputs, so that all correlations are inherited from the stimulus, then this term would be zero and the neuron at the center of our analysis would be completely redundant with the other K neurons, $\Delta I(\sigma_0;\mathbf{s}) = 0$. Stated in a more positive way, the global correlation structure of the retinal population is such that the extra information carried by individual neurons depends entirely on their departure from conditional independence. Although there is ample experimental evidence for these correlations [34], conditional independence remains a widely held intuition; our analysis indicates that the retina is far from this regime.

As a further test of these ideas we have looked at experiments on a very different network of neurons, in the mouse hippocampus [22, 25]. The results, to be described elsewhere, are very much the same, but perhaps less surprising since maximum entropy models with only pairwise interactions already provide an excellent description of these data, matching the higher order correlations within experimental error [22]. In contrast, as emphasized in Ref [21], for the population of cells in the retina the pairwise models show small but significant deviations from the data, and this has led to the exploration of several alternatives [21, 35, 36]. The point of our discussion is not to identify the correct model, but to understand why *any* simple model can succeed. Previous work has focused on simple forms of the interactions, taking intuition both from physics and from neurobiology. The arguments given here suggest, strongly, that what is essential for a simplified description is the compressibility of interactions [27].

We thank our experimental colleagues D Amodei, MJ Berry II, CD Brody, JL Gauthier, O Marre, and DW Tank for sharing the data of Refs [21, 22, 25], and we acknowledge helpful discussions with M Bauer, R Dickman, SE Palmer, and DJ Schwab. Work supported in part by the National Science Foundation through the Center for the Physics of Biological Function (PHY–1734030), the Center for the Science of Information (CCF–0939370), and PHY–1607612; and by the National Institutes of Health, through the BRAIN initiative (1R01EB026943).

[1] E Lubeck and L Cai, Single–cell systems biology by super–resolution imaging and combinatorial labeling. *Nat Methods* **9,** 743–748 (2012).

[2] AM Klein et al, Droplet barcoding for single cell transcriptomics applied to embryonic stem cells. *Cell* **161,** 1187–1201 (2015).

[3] EZ Macossko et al, Highly parallel genome–wide expression profiling of individual cells using nanoliter droplets. *Cell* **161,** 1202–1214 (2015).

[4] KH Chen, AN Boettiger, JR Moffitt, SS Wang, and X Zhuang, Spatially resolved, highly multiplexed RNA profiling in single cells. *Science* **348,** aaa6090–1 (2015).

[5] R Segev, J Goodhouse, J Puchalla, and MJ Berry II, Recording spikes from a large fraction of the ganglion cells in a retinal patch. *Nat Neurosci* **7,** 1154 –1161 (2004).

[6] DA Dombeck, CD Harvey, L Tian, LL Looger, and DW Tank. Functional imaging of hippocampal place cells at cellular resolution during virtual navigation. *Nat Neurosci* **13,** 1433–1440 (2010).

[7] O Marre, D Amodei, N Deshmukh, K Sadeghi, F Soo, TE Holy, and MJ Berry II, Mapping a complete neural population in the retina. *J Neurosci* **32,**14859–14873 (2012).

[8] MB Ahrens, MB Orger, DN Robson, JM Li, and PJ Keller, Whole-brain functional imaging at cellular resolution using light–sheet microscopy. *Nat Methods* **10,** 413–420 (2013).

[9] JJ Jun et al, Fully integrated silicon probes for high–density recording of neural activity. *Nature* **551,** 232–236 (2017).

[10] JE Chung et al, High–density, long–lasting, and multi–region electrophysiological recordings using polymer electrode arrays. *Neuron* **101,** 21–31 (2019).

[11] A Cavagna and I Giardina, Bird flocks as condensed matter, *Annu Rev Condens Matter Phys* **5,** 183–207 (2014).

[12] Y LeCun, Y Bengio, and G Hinton, Deep learning. *Nature* **521,** 436–444 (2015).

[13] BM Yu, JP Cunningham, G Santhanam, SI Ryu, KV Shenoy, and M Sahani, Gaussian–process factor analysis for low–dimensional single–trial analysis of neural population activity. *J Neurophysiol* **102,** 614–635 (2009).

[14] JA Gallego, MG Perich, LE Miller, and SA Solla, Neural manifolds for the control of movement. *Neuron* **94,** 978–984 (2017).

[15] MK Transtrum, BB Machta, KS Brown, BC Daniels, CR Myers, and JP Sethna, Perspective: Sloppiness and emergent theories in physics, biology, and beyond. *J Chem Phys* **143,** 010901 (2015).

[16] KN Quinn, H Wilber, A Townsend, and JP Sethna, Chebyshev approximation and the global geometry of model predictions. *Phys Rev Lett* **122,** 158302 (2019).

[17] E Schneidman, MJ Berry II, R Segev, and W Bialek, Weak pairwise correlations imply strongly correlated network states in a neural population. *Nature* **440,** 1007–1012 (2006); arXiv:q–bio.NC/0512013 (2005).

[18] W Bialek and R Ranganathan, Rediscovering the power of pairwise interactions. arXiv:0712.4397 [q–bio.QM] (2007).

[19] M Weigt, RA White, H Szurmant, JA Hoch, and T Hwa, Identification of direct residue contacts in protein-protein interaction by message passing. *Proc Natl Acad Sci (USA)* **106,** 67–72 (2009).

[20] DS Marks, LJ Colwell, R Sheridan, TA Hopf, A Pagnani, R Zecchina, and C Sander, Protein 3D structure computed from evolutionary sequence variation. *PLoS One* **6,** e28766 (2011).

[21] G Tkačik, O Marre, D Amodei, E Schneidman, W Bialek, and MJ Berry II, Searching for collective behavior in a large network of sensory neurons. *PLoS Comput Biol* **10,** e1003408 (2014); arXiv:1306.3061 [q–bio.NC] (2013).

[22] L Meshulam, JL Gauthier, CD Brody, DW Tank, and W Bialek, Collective behavior of place and non-place neurons in the hippocampal network. *Neuron* **96,** 1178–1191 (2017).

[23] HC Nguyen, R Zecchina, and J Berg, Inverse statistical problems: from the inverse Ising problem to data science. *Adv Phys* **66,** 197–261 (2017).

[24] A Cavagna, I Giardina, and T Grigera, The physics of flocking: Correlation as a compass from experiments to theory. *Phys Repts* **728,** 1–62 (2018).

[25] L Meshulam, JL Gauthier, CD Brody, DW Tank, and W Bialek, Coarse–graining, fixed points, and scaling in a large population of neurons. *Phys Rev Lett* **123,** 178103 (2019).

[26] GB Morales, S Di Santo, and MA Muñoz, Quasi–universal scaling in mouse brain neuronal activity stems from edge–of–instability critical dynamics. arXiv:2111.12067 [cond–mat.stat–mech] (2021).

[27] W Bialek, SE Palmer, and DJ Schwab, What makes it possible to learn probability distributions in the natural world? arXiv:2008.12279 [cond–mat.stat–mech] (2020).

[28] N Tishby, FC Pereira, and W Bialek, The information bottleneck method. In *Proceedings of the 37th Annual Allerton Conference on Communication, Control and Computing,* B Hajek and RS Sreenivas, eds, pp 368–377 (University of Illinois, 1999); arXiv:physics/0004057 (2000).

[29] TM Cover and JA Thomas, *Elements of Information Theory* (Wiley, New York, 1991).

[30] LP Kadanoff, Scaling laws for Ising models near T_c. *Physics* **2,** 263–272 (1966).

[31] J Cardy, *Scaling and Renormalization in Statistical Physics* (Cambridge University Press, Cambridge UK, 1996).

[32] SP Strong, R Koberle, RR de Ruyter van Steveninck, and W Bialek, Entropy and information in neural spike trains. *Phys Rev Lett* **80,** 197–200 (1998).

[33] N Brenner, SP Strong, R Koberle, W Bialek, and RR de Ruyter van Steveninck, Synergy in a neural code. *Neural Comp* **12,** 1531–1552 (2000).

[34] For a review see the Supplementary Information in G Tkačik, T Mora, O Marre, D Amodei, SE Palmer, MJ Berry II, and W Bialek, Thermodynamics and signatures of criticality in a network of neurons. *Proc Natl Acad Sci (USA)* **112,** 11508–11513 (2015).

[35] E Ganmor, R Segev, and E Schneidman, Sparse low–order interaction network underlies a highly correlated and learnable neural population code. *Proc Natl Acad Sci (USA)* **108,** 9670–9684 (2011).

[36] J Humplik and G Tkavšik, Probabilistic models for neural populations that naturally capture global coupling and criticality. *PLoS Comput Biol* **13,** e1005763 (2017).